THE JOURNAL OF PHYSICAL CHEMISTRY B

Article

pubs.acs.org/JPCB

Design, Synthesis, Physicochemical Studies, Solvation, and DNA Damage of Quinoline-Appended Chalcone Derivative: Comprehensive Spectroscopic Approach toward Drug Discovery

Himank Kumar,[†] Anjan Chattopadhyay,[‡] R. Prasath,[‡] Vinod Devaraji,[§] Ritika Joshi,[†] P. Bhavana,[‡] Praveen Saini,[‡] and Sujit Kumar Ghosh*[,†]

[†]Department of Chemistry, Visvesvaraya National Institute of Technology, Nagpur, Maharashtra 440010, India

[‡]Department of Chemistry, BITS-Pilani, K. K Birla Goa Campus, Zuarinagar, Goa 403726, India

[§]Department of Pharmaceutical Chemistry, College of Pharmacy, Madras Medical College, Chennai 600003, India

Supporting Information

ABSTRACT: The present study epitomizes the design, synthesis, photophysics, solvation, and interaction with calf-thymus DNA of a potential antitumor, anticancer quinoline-appended chalcone derivative, (*E*)-3-(anthracen-10-yl)-1-(6,8-dibromo-2-methylquinolin-3-yl)prop-2-en-1-one (ADMQ) using steady state absorption and fluorescence spectroscopy, molecular modeling, molecular docking, Fourier-transform infrared spectroscopy (FTIR), molecular dynamics (MD) simulation, and gel electrophoresis studies. ADMQ shows an unusual photophysical behavior in a variety of solvents of different polarity. The dual emission has been observed along with the formation of twisted intramolecular charge transfer (TICT) excited state. The radiationless deactivation of the TICT state is found to be promoted strongly by hydrogen bonding. Quantum mechanical (DFT, TDDFT, and ZINDO−CI) calculations show that the ADMQ is sort of molecular rotor which undergoes intramolecular twist followed by a complete charge transfer in the optimized excited state. FTIR studies reveals that ADMQ undergoes important structural change from its native structure to a β-hydroxy keto form in water at physiological pH. The concentration-dependent DNA cleavage has been identified in agarose gel DNA electrophoresis experiment and has been further supported by MD simulation. ADMQ forms hydrogen bond with the deoxyribose sugar attached with the nucleobase adenine DA-17 (chain A) and result in significant structural changes which potentially cleave DNA double helix. The compound does not exhibit any deleterious effect or toxicity to the *E. coli* strain in cytotoxicity studies. The consolidated spectroscopic research described herein can provide enormous information to open up new avenues for designing and synthesizing chalcone derivatives with low systematic toxicity for medicinal chemistry research.

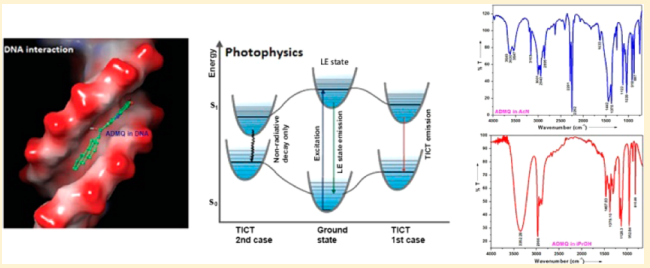

INTRODUCTION

Synthesis of small molecule, its binding with DNA, and the recognition of DNA sequences are of immense interest in the arena of medicinal chemistry.[1−5] In view of the urge for searching new promising small therapeutic agents, we hereby introduce quinoline-appended anthracenyl chalcone. Chalcones are α, β-unsaturated ketones, biogenetic precursors of flavonoids in higher plants. They are intermediates and end products of flavonoid biosynthesis and starting material for the synthesis of different types of highly bioreactive heterocyclic compounds, such as pyrazolines, pyrimidines, thiophenes, etc. Chalcones may exist in cis and trans isomeric forms, of which the trans form is thermodynamically favorable.[6] Clinical trials have shown that chalcones reached reasonable plasma concentration and did not cause any toxicity.[7] Chalcones display a wide range of pharmacological properties, including cytotoxity toward cancer cell lines.[7,8] Functional groups on the two aromatic rings influences to a certain degree of specific biological activities.[9] In this regard, chalcones containing heterocycles and chromophores are of particular interest and several such compounds have been investigated.[6] Among the nitrogen heterocycles, quinolines and their derivatives have outstanding biological significance.[10] They are found to form the basis of many drugs used in the treatment of cancer and inflammatory diseases,[11] antibacterial, antiviral, antineoplastic, antiischemic, antiallergic, antihypertensive, and antiulcerative agents.[9,12] Anthracene-appended molecules are also reported to have a broad spectrum of photophysical and biological properties like topoisomerase II inhibition and interaction with DNA and human serum albumin.[13] However, quinoline-appended anthraceneyl chalcone compounds are unexplored to the best of our knowledge. Although quinolinyl chalcones shows antimalarial, antibacterial, antifungal properties,[9] and cytotoxicity to cancer cell lines,[8] the exact mechanism of its

Received: March 13, 2014
Revised: June 10, 2014

dx.doi.org/10.1021/jp5025262 | J. Phys. Chem. B XXXX, XXX, XXX−XXX

bioactivity is still unknown and this has left a gap in the chalcone-based drug designing. Higher bioactivity and rich photophysical properties[14] of quinolinyl chalcone derivatives, depending on the substitution pattern on the aryl rings, make them prime candidates as probes to monitor their binding interaction with the biomacromolecules, their uptake, and localization within the cell without the use of costaining.

In this paper, we hereby demonstrate the design, synthesis of a chalcone derivative, its detailed physicochemical studies, solvation coupled with DNA recognition, and characterization of its interaction in a single comprehensive article, which is significantly fascinating as this may provide enormous and effective information for designing more efficient chalcone-based therapeutic agents, in controlling gene expression for the medicinal chemistry research.

EXPERIMENTAL SECTION

Materials and Sample Preparation. 2-Amino-3,5-dibromobenzaldehyde, acetylacetone, and calf thymus DNA (ct DNA) was procured from Sigma-Aldrich (St. Louis, MO). *N*-[2-Hydroxyethyl] piperazine *N*-[2-ethanesulfonic acid] (HEPES) buffer and ethidium bromide (EtBr) were obtained from SRL, India. Agarose for nucleic acid electrophoresis (DNase, RNase Free), TAE buffer (4.84 g Tris base, pH 8.0, 0.5 M EDTA/L), and standard DNA molecular weight marker (λ DNA/Hind III digest) was purchased from Merck, India. The spectroscopic grade solvents *n*-heptane, hexane, 1,4-dioxane, tetrahydrofuran, choloroform, dichloromethane, dimethylformamide, acetonitrile, isopropyl alcohol, ethyl alcohol, and methyl alcohol were used as received (Fischer-scientific, India).

Stock solution of ct DNA was prepared by dissolving solid ct DNA in 50 mM HEPES Buffer (pH 7) and stored at 4 °C. The concentration of DNA solution was determined spectrophotometrically using ϵ_{DNA} = 13600 mol^{-1} dm^3 cm^{-1} at 260 nm. Concentrated stock solution of ADMQ was prepared in spectroscopic-grade 1,4-dioxane, and 10 μL of the same solution was added in to 5 mL of different solvents for the measurement. The molar extinction coefficient and the quantum yield of ADMQ in dioxane are 1.0719 × 10^4 L mol^{-1} cm^{-1} (at 414 nm) and 0.14, respectively. The quantum yield of fluorescein (ϕ = 0.93)[14] was used as reference for the quantum yield measurement of the sample. Millipore water was used to prepare solutions wherever required.

Instrumentation and Methodology. *UV−vis Absorption and Emission Study.* UV−vis absorption measurements were performed at room temperature with JASCO V-630 Bio Spectrophotometer with a matched pair of quartz cuvettes, and steady state fluorescence spectra was recorded on a JASCO FP-8300 spectrofluorometer using 1.0 cm quartz cell and an external slit width of 2.5 nm. An excitation wavelength corresponding to the lowest energy band of ADMQ in solvents was chosen and appropriate blanks were subtracted to correct the background. Measurements were repeated in order to obtain reproducible results.

The purity of ct DNA was verified by monitoring the ratio of absorbance at 260 nm to that of 280 nm, which was in the range of 1.76−1.8, indicating that ct DNA is satisfactorily free from proteins. Steady state photolysis was performed under white light illumination for 30 s interval and the corresponding absorption spectra were measured using JASCO V-630 Bio spectrophotometer with a matched pair of quartz cuvettes.

Time-Resolved Fluorescence Measurements. Time-resolved fluorescence measurements were performed by time-correlated single-photon counting (TCSPC) method using a picosecond diode laser at 403 nm (IBH Nano LED) as a light source with a TBX-04 detector (all IBH, U.K.). The data stored in a multichannel analyzer were routinely transferred to the IBH DAS-6 decay analysis software.

Elemental Analysis. Elemental analysis was performed on an Elementar Vario EL III elemental analyzer. The 1H NMR spectra was recorded on Bruker AVANCE III-500 MHz spectrometers in deuterated chloroform ($CDCl_3$), with tetramethylsilane as an internal standard. ESI mass spectra were recorded on a Micromass Quarto II mass spectrometer.

FTIR Study. FTIR spectra were recorded on a Shimadzu IR Affinity-1 spectrophotometer, equipped with DTGS (deuterated triglycine sulfate) detector and KBr beam splitter assembly. Liquid sample were tightly packed in a liquid cell made up of two ZnSe windows for infrared measurements. Forty-five scans were accumulated for each sample in the spectral range of 4000−400 cm^{-1} with a resolution of 4 cm^{-1}. Background spectra were collected before each measurement. All the measurements were carried out at room temperature and a controlled ambient humidity of 45% RH. A spectrum of solvent was recorded and subtracted from ADMQ spectrum. Repeated measurements were done to check the reproducibility. All FTIR spectra was blank corrected as reported otherwise.

Cytotoxicity Studies. The *Escherichia coli AB 1157*, a wild-type strain was considered for cytotoxic study. The stock culture of bacteria was revived by inoculating in broth medium (Tryptone-10 g, NaCl-10g, yeast extract, 5 g, and Agar, 20 g in 1000 mL of distilled water) and grown at 37 °C for 18 h. The LB Agar plates were prepared and wells were made in the solidified LB agar plate. Each plate was inoculated with 18 h old culture (100 μL, 10^{-4} cfu) spread evenly on the plate. After 20 min, the wells were filled with compound at different concentrations. A similar method was used for the standard compound plate of Stannous Chloride. All the plates were incubated at 37 °C for 24 h, and the diameter of inhibition zone was noted.

Agarose Gel DNA Electrophoresis and Gel Documentation. Gel electrophoresis was carried out using mini horizontal subcell GT electrophoresis system equipped with PowerPac basic power supply. ADMQ at various concentrations was added to the reaction mixture containing ct DNA in 50 mM HEPES Buffer, pH 7. After incubation at 37 °C for 12 h, loading buffer (0.25% bromophenol blue, 0.25% xylene cyanol, 30% glycerol in water) was added to each tube and the solution was loaded onto a 1% agarose gel. The electrophoresis was carried out for ∼45 min at 50 V in TAE buffer (4.84 g Tris base, pH 8.0, 0.5 M EDTA/1 L). Gel was stained with EtBr (10 μg/mL) prior to being photographed using Molecular Imager Gel Doc XR (Biorad Laboratories) consisting of UV trans-illuminator and camera image so obtained was assessed using Image Lab software.

In Silico Studies. The computational studies were carried out using Windows 7 professional, 64 bit Intel core i5−2500 CPU at 3.30 GHz, 4 GB RAM) using the Schrödinger 2013 suite.

Ligand and DNA Preparation. The synthesized ligands different forms (Native ADMQ, form II, and form III) were sketched in maestro 9.3 (Maestro, version 9.2, Schrödinger, LLC, New York, NY, 2011), and prepared by ligprep (LigPrep, version 2.7, Schrödinger, LLC, New York, NY, 2013) to rectify

dx.doi.org/10.1021/jp5025262 | J. Phys. Chem. B XXXX, XXX, XXX−XXX

Scheme 1. Synthesis of ADMQ

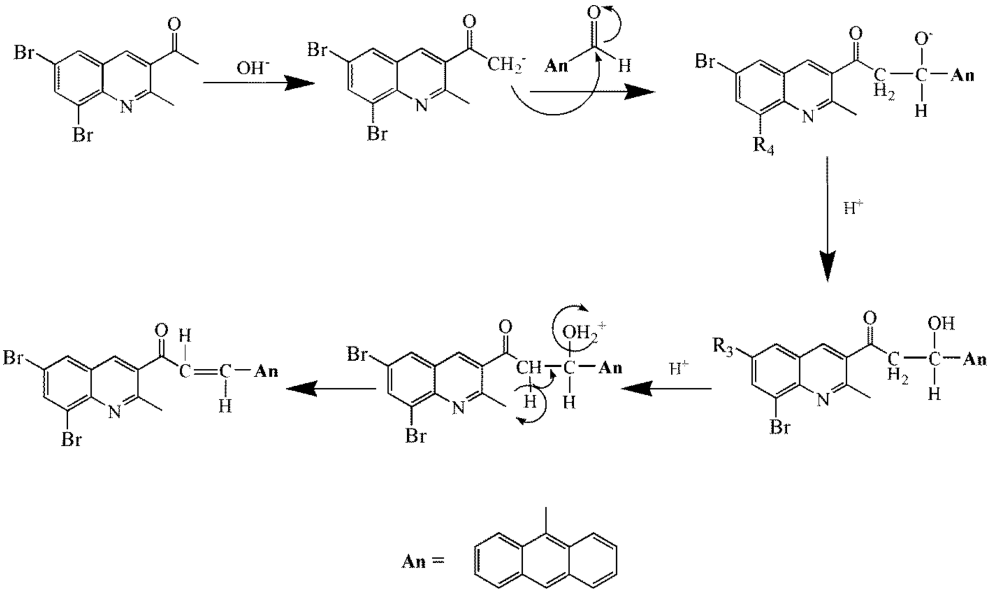

the molecular geometries, and to get least energy conformations. As the study is against DNA, we selected the DNA [d (CGTTTTTACG): d (CGTAAAAACG)] from the protein data bank (PDB ID: 226D). This structure was selected on the basis of its AT content in agreement with the ct DNA, used in agarose gel electrophoresis. The double helical DNA strand was prepared by minimizing truncated newton algorithm with energy and gradient convergence criteria by using impact (Impact, version 6.0, Schrödinger, LLC, New York, NY, 2013) with distance-dependent electrostatic potential using force field 2005. The minimized DNA grid was specified by Glide receptor grid generation using centroid of crystal native ligand with van der Waals cut off for receptor sites with the nonpolar atoms setup to 0.8 and partial charge adjusted to 0.25 in such a way that both minor and major groove of DNA was covered.

Molecular Docking and Binding Energy Calculation. The molecular docking was carried out by glide docking (Glide, version 6.0, Schrödinger, LLC, New York, NY, 2013)using an extra precision mode, which utilizes as an input the prepared ligand and grid generated in the earlier steps and ligand sampling as flexible for docking against the biological target. Here the interaction pattern, glide energy, and docking score of the synthesized compound against the DNA were studied. The binding energy calculation was carried out by Prime Molecular Mechanics/Generalized Born Surface Area MM-GBSA (Prime, version 3.3, Schrödinger, LLC, New York, NY, 2013) that calculates ligand binding energies and ligand strain energies for a set of ligands and DNA. The pose viewer file generated by the glide extra precision docking pose file was used as an input for the calculation of solvation model VSGB (variable-dielectric generalized Born model) followed by minimization.

Molecular Dynamics Simulation. The compound which gave best pose complex against DNA was considered for molecular dynamics to understand the atomic level interaction and stability of the complex. To build the system, we used Desmond (Desmond Molecular Dynamics System, version 2.2, D. E. Shaw Research, New York, NY, 2009. Maestro-Desmond Interoperability Tools, version 2.2, Schrödinger, New York, NY, 2009) system builder using explicit water solvation SPC model with cubic box size by box size calculation method as absolute size with box volume 117327 A^3 with OPLS force field 2005. The system was then minimized using a maximum of 2000 iterations with convergence threshold of 1.0 kcal/mol A^3. The in silico simulation of the system with a simulation time of 10 ns with recording interval of energy 1.2 and trajectory of 4.8 using NPT ensemble of temperature 300 K and pressure of 1.01325 bar was carried out for synthesized ADMQ (form II) and intercalator EtBr.

Synthesis of ADMQ. The precursor of the chalcone 1-(6,8-dibromo-2-methylquinolin-3-yl)ethanone is synthesized by Friedlander cyclization of substituted 2-aminoacetophenone with acetylacetone in acidic medium.[15] Synthesis of chalcone is carried out by Claisen-Schmidt condensation of 1-(6,8-dibromo-2-methylquinolin-3-yl)ethanone with the 9-anthracenecarboxaldehyde using potassium hydroxide as a catalyst in ethanol. The reaction time is determined by monitoring the consumption of starting materials as indicated by TLC. The synthesized quinoline-appended chalcone (via the Claisen-Schmidt condensation) leads to the exclusive formation of the *E*-configuration, which is a result of the more favorable antiperiplanar elimination of the hydroxide group from the carbanion intermediate.[14,15] The predominance of the *E*-configuration of the C═C bond in chalcones has been established via ^{1}H NMR spectroscopy. Yield: 74%. IR (KBr) cm^{-1}: 1674 (C═O), 1621 (C═C); ^{1}H NMR (500 MHz, $CDCl_3$) δ: 3.05 (s, 3H, $-CH_3$), 7.28 (d, 16.0 Hz, 1H, H_α), 7.53−7.59 (m, 4H, Ar−H), 8.00 (d, J = 2.0 Hz, 1H, Ar−H), 8.06 (d, J = 8.0 Hz, 2H, Ar−H), 8.23 (d, J = 12.0 Hz, 2H, Ar−H), 8.24 (s, 1H, Ar−H), 8.33 (s, 1H, Ar−H), 8.53 (s, 1H, Ar−H), 8.60 (d, 16.0 Hz, 1H, H_β), ESI-MS calculated for $[M + H]^+$: 531.97; found: 532.10. Elemental analysis for $C_{27}H_{17}Br_2NO$: C, 61.04; H, 3.23; N, 2.64%; Found: C, 61.45; H, 3.49; N, 2.26%.

RESULTS AND DISCUSSION

Design and Synthesis. Open-chain flavonoids where the two aromatic rings are joined by a three carbon chain (1,3-diphenyl-2-propen-1-one) can be synthesized with various structural variants (Scheme 1). Tuning the substitution pattern on the two aromatic rings, a wide range of pharmacological

dx.doi.org/10.1021/jp5025262 | J. Phys. Chem. B XXXX, XXX, XXX−XXX

activities can be identified for specific targets in the human body.[15] Hence, a complete understanding of the mechanism and the structural requirements for its specific biological activity is essential in guiding and optimizing its design.

Scheme 2. General Structure of Chalcone

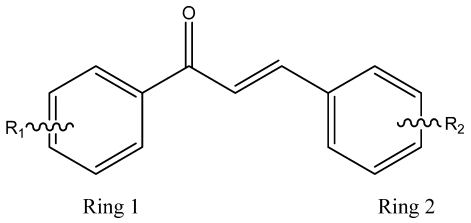

Among numerous structural possibilities, we have substituted an aryl group by heterocyclic quinoline derivative (as ring 1) and the other group by bioactive anthracene derivative (as ring 2) to enhance its biological activity as a whole. This has been attempted to design a sort of molecular rotor[16] with three linked units, an electron donor unit (D), an acceptor unit (A), and an electron-rich spacer unit with alternate single and double bonds ($D^+\cdots\pi\cdots A^-$). The detail molecular docking studies of several such compounds have been performed (S1) substituting different heterocycles attached with the main pharmacophore. The above said design has been finalized considering synthetic feasibility and on triumph of in silico MM-GBSA binding energy of −41.7209 kcal/mol with DNA (for the most stable ADMQ conformer) to ensure the possibility of its bioactive interaction in vitro/in vivo.

Photophysics. *Steady State Absorption and Emission Study.* The steady state absorption and emission measurement of this newly synthesized quinoline-appended chalcone (ADMQ) has been studied in different solvents with varying polarity, viz., *n*-hexane, *n*-heptane, benzene, 1,4-dioxane, tetrahydrofuran, chloroform, dichloromethane, dimethylformamide, acetonitrile (ACN), tert-butanol, isopropanol, *n*-butanol, ethyl alcohol, methyl alcohol, and water. ADMQ shows two different absorption bands at 252 and 414 nm in *n*-hexane. Increase in the solvent polarity from nonpolar to aprotic polar does not induce loss in the structure of absorption band, and there is hardly any significant change in the absorption maxima upon changing the solvent polarity. This ruled out the formation of the charge transfer character of ADMQ in the ground state (G.S.) in aprotic solvents. However, the interaction of ADMQ with protic polar solvents, especially in water, shows a substantial (15 nm) red shift in absorption maxima (ascribed to the H-bonding), followed by protonation with consequent structural change of ADMQ in the G.S., as discussed later.

ADMQ exhibits considerable dual emission while exciting at the lowest-energy band. The molar extinction coefficient and the quantum yield of ADMQ in dioxane are 1.0719×10^4 L mol^{-1} cm^{-1} (at 414 nm) and 0.14, respectively. In alkane, ADMQ gives a structured emission showing a mirror image relationship with the corresponding absorption spectrum. Hence in alkane, the emission maxima at 495 nm, originate from locally excited (LE) species with a shoulder at 535 nm. With the increase in solvent polarity, the lowest energy emission band (at 535 nm) predominates over the LE band, and a red shift in fluorescence maxima from 535 to 552 nm has been observed (Figure 1a) with a significant decrease in the fluorescence intensity (Figure 1b). The unusual photophysical behavior (Figure 1c) and the 17 nm bathochromic shift of the

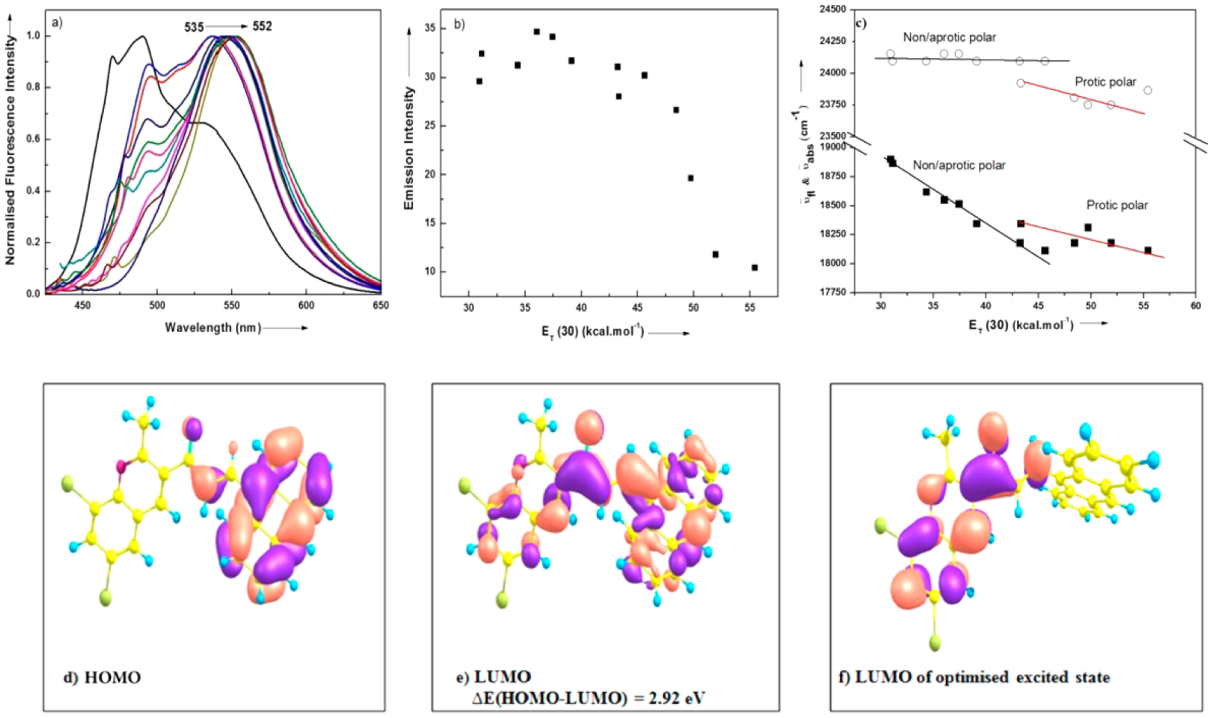

Figure 1. (a) Normalized fluorescence spectrum of ADMQ in different solvents with increasing polarity. (b) Plot of emission intensity (of red-shifted second emission band) vs $E_T(30)$ (kcal/mol) in different solvents. (c) Dependence of absorption wavenumber and the emission wavenumber maxima of TICT state with solvent polarity parameter $E_T(30)$ (kcal/mol). (d) HOMO and (e) LUMO of ADMQ (form I) at the ground state geometry (f) LUMO of ADMQ (form I) at the optimized excited state (twisted) geometry calculated at the B3LYP/6-31G* level.

dx.doi.org/10.1021/jp5025262 | J. Phys. Chem. B XXXX, XXX, XXX−XXX

Scheme 3. Structural Change of ADMQ in Different Environments

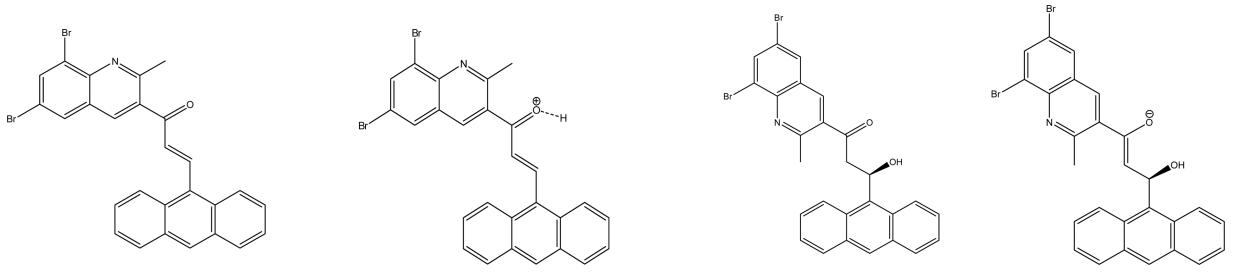

Table 1. Predicted Absorption Peak Positions of the Chloro Analogues of ADMQ at ZINDO−CI and ZINDO/RPA Level

compound	methods	predicted absorption peak (nm)	oscillator strength	predicted absorption peak (nm)	oscillator strength
chloro analogue of form I	ZINDO−CI	392	0.53	258	1.58
	ZINDO-RPA	403	0.44	268	1.29
chloro analogue of form II	ZINDO−CI	410	0.63	264	0.80
	ZINDO-RPA	422	0.50	274	1.03
chloro analogue of form III	ZINDO−CI	345	0.29	250	2.46
	ZINDO-RPA	360	0.21	262	1.93
chloro analogue of form IV	ZINDO−CI	544	0.16	248	1.80
	ZINDO-RPA	547	0.15	259	1.89

emission maxima with solvent polarity indicates the stabilization of the excited states (E.S.) primarily due to formation of an intramolecular charge transfer (ICT), which finally leads to more stable twisted intramolecular charge transfer (TICT) state (discussed in later section).

Photoisomerisation of certain chalcones are reported in literature.[17,18] Photoisomerization reaction which usually involves an intersystem crossing (ISC), is one of the process that may take place in the E.S. in competition with other processes.[17] The possibility of photoisomerization reaction of ADMQ has been experimented (in methanol and in dioxane) with white light illumination of 30 s interval. The absorption spectrum does not show the formation of any new band during photolysis. Moreover, in the competition between TICT and photoisomerization, the solvent-induced stabilization of the TICT state may drive the population from the LE state toward the charge transfer state giving less chance for the other competing channel (photoisomerization) to dominate. The observed intense TICT emission peaks of ADMQ clearly support this possibility. The above two experimental evidences (photolysis and intense TICT emission) indicate the possible nondominant behavior of the photoisomerization in competition with the charge transfer reaction of ADMQ.

Theoretical Calculations. Density functional theory (DFT) and ZINDO-CI-based quantum mechanical calculations have been attempted to vindicate the above experimental observations. The structure of ADMQ (form I, Scheme 3) has been optimized at the DFT/B3LYP level of theory with the 6-31G (d) basis set. The presence of a comparatively smaller C−C bond (1.48 Å) has been found in the G.S. in the central enone part of the system which links the anthracene moiety to the quinoline moiety. The charge in the HOMO species is almost exclusively distributed over the anthracene moiety (Figure 1d), and we noticed a clear indication of its transfer to the left side from HOMO to LUMO (Figure 1e). The HOMO−LUMO gap in this species is found to be 2.91 eV. Since in charge transfer systems the vertical excitation energy from the TDDFT method gives a highly overestimated value, the ZINDO/CI technique has also been employed for a better estimation of vertical excitation energy using Arguslab. However, the bromo-substituted species is not compatible with the UV−vis excitation energy calculation in the mentioned software; hence, the corresponding chloro system has been tested as an alternative and which is found to give almost similar geometrical features (verified by DFT run) and charge separation behavior as our investigated compound. The results are shown in Table 1 and clearly found to be in-line with the results obtained for the actual bromo compound in DFT calculations. The ZINDO/RPA method has also been employed for the calculation of UV−vis parameters. As per the experimental observation for the bromo species, a peak around 410 nm of lower intensity (low oscillator strength) has been found (Table 1) for its chloro analogue, too, which arises due to the HOMO → LUMO excitation. The more intense peak is found around 260 nm arising from a mixed contribution from several configurations, such as HOMO-1 → LUMO. These results are consistent with the experimental steady state absorption peaks of ADMQ obtained in the nonpolar medium.

Environmental Effect on the Excited States. The environmental effect in the cybotactic region of ADMQ shows a unique photophysical behavior. Distinct plot of the absorption wavenumber and the emission wavenumber maxima of the TICT state have been plotted with solvent polarity parameter $E_T(30)$ (Figure 1c). An unusual two different linearity with dissimilar slopes have been observed in aprotic and in protic solvents for both cases. Similar unusual photophysical behaviors have been reported earlier for intramolecular charge transfer systems and isomeric (phenylamino)naphthalene-sulfonates,[19,20] TICT probe dimethylamino-benzonitrile (DMABN),[21,22] and coumarin systems.[23,24] ADMQ is involved

dx.doi.org/10.1021/jp5025262 | J. Phys. Chem. B XXXX, XXX, XXX−XXX

in strong solute−solvent H-bond interactions in protic solvents, which induces significant red shifts of the absorption spectra with respect to nonprotic solvents. Such red shifts of the absorption spectrum typically correspond to a strengthening of the solute−solvent H-bonds in the LE state. Both G.S. and E.S. may undergo such H-bonding; however, this can affect the stability of these states in a different manner depending on their respective charge separations. The excited state of ADMQ will be more stabilized, especially at the TICT state, as the LUMO (Figure 1, panels e and f) are having higher electronic cloud on the carbonyl oxygen in comparison to the HOMO.

Planar ICT to TICT Conversion. The red shift of the emission peak and the decrease in the fluorescence intensity of ADMQ with change in the solvent polarity from nonpolar to polar (Figure 1, panels a and b) can be explained from the conversion of the excited planar ICT state to the TICT state. ADMQ seems to be a sort of molecular rotor which undergoes an intramolecular twist in the fluorescent excited state. This molecular rotor[16] consists of three linked units, an electron donor unit (anthracene moiety), an acceptor unit (quinoline moiety), and an electron-rich spacer unit (enone part), which includes alternate single and double bonds ($D^+\cdots\pi\cdots A^-$). This spacer unit facilitates electron movement by bringing the donor and acceptor units in conjugation with minimum overlap of their respective orbitals. For a donor−acceptor system like ADMQ, the Jablonski diagram may be extended with two possible varieties of relaxation of the twisted state. The first possibility is appearance of a distinct second emission band that is red-shifted from the LE fluorescence band. This usually happens when the S_1-S_0 energy gap in the twisted state is sufficiently large enough to allow photon emission; however, this gap is substantially lower than that in the LE state. Relaxation from both LE and twisted conformation takes place, resulting in two emission peaks. The twisted conformation may have a more intense peak if the LE-to-TICT transformation is allowed, which has actually been observed experimentally for ADMQ in aprotic and polar solvents, but if the TICT state is not favored, LE emission predominates over it (in alkane). In the second possibility, if the twisted energy gap is much smaller than the LE energy gap, or in this case, the conical intersection/vibronic coupling takes place between the two states, the nonradiative emission occurs exclusively from the twisted conformation. Overall, the twisted geometry opens up a nonradiative relaxation channel with the appearance of a red-shifted second emission band, which practically dominates the LE emission band.

When ADMQ is exposed to the different solvents from nonpolar hexane to aprotic polar ACN and finally to alcohols, the fluorescence intensity of red-shifted second emission band has been decreased. This reduction in the fluorescence intensity in the alcoholic medium indicates the fact that the H-bonding dynamics in these fluorescent TICT states is probably playing an important role for this quenching process.[25−27] The internal conversion probably gets promoted due to a change of the H-bonding strength between the ground and the excited states. Since polar solvents stabilize the ICT state, and hence, it also stabilizes the TICT state and thus increases the relaxation time of the TICT state.[28] The polarity of molecules is also associated with the ability to form H-bond, and this H-bond formation between molecular rotors and the solvent increases the TICT formation rate. Molecular rotors like ADMQ typically exhibit stronger solvatochromism in the twisted-state emission band than in the planar locally excited (LE) emission band because of the larger charge separation of the excited states.[16] Furthermore, both the G.S. and the E.S. energy levels depend on the degree of intramolecular rotation.[29] In G.S., a planar conformation is energetically preferred, whereas the twisted conformation is the preferred conformation in the E.S. Therefore, the excited molecule rapidly assumes the twisted-state conformation, which has been further confirmed theoretically by optimization of the first excited state of ADMQ at the TDDFT/B3LYP level. Analysis of the LUMO of the optimized excited state shows that exclusive charge transfer has occurred from the anthracene to the left-hand side moiety (Figure 1f). It is quite interesting that the anthracene moiety is found to rotate and becomes almost perpendicular to the quinoline ring and the middle part of the molecule. This observation clearly indicates that the E.S. is likely to undergo a change from the planar ICT to the TICT state after the photoexcitation. The charge transfer is highly facilitated by the polar solvents, and there is a possibility of complete (100%) charge transfer in those solvents. This intramolecular twist opens the nonradiative decay channel; as soon as the twist starts, the fluorescence yield drops as it has actually been observed experimentally in different solvents (Figure 1b). This ICT-to-TICT conversion mechanism seems to be acting strongly in case of alcoholic (protic) solvents and to some extent in the aprotic polar solvents too. However, in the case of water, the TICT conversion does not take place probably because of the structural change of ADMQ in water, which will be explained in detail later.

Solvation in Alcohols. *Radiationless Deactivation of TICT Promoted by Hydrogen Bonding.* Alcohol molecules not only exhibit substantial specific solvation of the excited state but also induce efficient radiationless deactivation.[30,31] The molecular mechanism of solvent relaxation followed by a radiationless process is strongly dependent on the molecular structure and the microscopic electronic structural differences in the excited state.[28,32] The steady state absorption and emission behavior of ADMQ has been studied upon gradual addition of ethanol in benzene. It shows an appreciable amount of red shift (538 to 551 nm) of fluorescence maxima with significant fluorescence quenching. The typical fluorescence spectra have been shown in Figure 2. The dynamic aspect of fluorescence quenching behavior and it is efficiency has been determined using Stern−Volmer relation as

$$F_0/F = 1 + K_{sv}[\text{ethanol}] = 1 + k_q\tau[\text{ethanol}] \quad (1)$$

where F_0, F, K_{sv}, k_q and τ denote fluorescence intensity of ADMQ in benzene without ethanol, fluorescence intensity in benzene with ethanol, Stern−Volmer quenching constant, bimolecular rate constant, and fluorescence lifetime, respectively. Time-resolved emission spectra has shown the biexponential decay, a quick deactivation (τ_1 =53 ps) followed by the excited state lifetime (τ_2 = 1.86 ns) in ethanol. Using above excited state lifetime of ADMQ, the value of k_q has been calculated as 0.1438×10^9 M^{-1} s^{-1}. The magnitude of bimolecular rate constant (10^9) also supports the dynamic quenching behavior of the fluorophore. All these observations clarified by the H-bond assisted radiationless deactivation of a TICT excited state. In the presence of alcohol, both the ground (discussed in later section) and the excited states can form H-bonding with the solvents, but since the negative charge density on the acceptor part (quinoline and the carbonyl carbon) in the E.S is higher as noticed in TDDFT calculation (Figure 1f), a stronger H-bond is expected to be formed between the excited

dx.doi.org/10.1021/jp5025262 | J. Phys. Chem. B XXXX, XXX, XXX−XXX

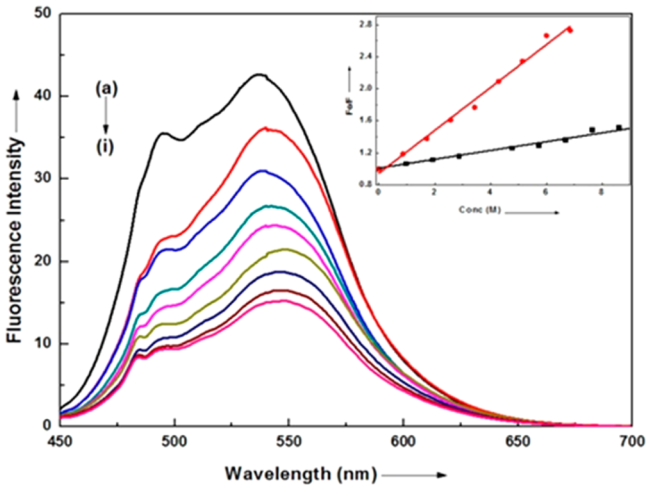

Figure 2. Fluorescence spectra of ADMQ in benzene on gradual addition of ethanol at 298 K. Curves (a–i) correspond to [EtOH] = 0.0, 0.85, 1.71, 2.57, 3.42, 4.28, 5.14, 6.00, 6.85 M, respectively. (Inset) Comparative Stern–Volmer fluorescence quenching plot in benzene on gradual addition of EtOH (●—●, red)/AcN (■—■, black) at 298 K.

molecule and the alcohol. This H-bond between the acceptor part in ADMQ and the ethanol is strengthened in the TICT state, which assists the deactivation of E.S. via internal conversion.[25] However, a dynamic equilibrium may exist between free ICT/TICT state and the H-bonded ICT/TICT state.

Radiationless Deactivation in Aprotic Solvents. A control experiment, the gradual addition of aprotic polar ACN in nonpolar benzene has also been performed to identify the role of H-bonding with an electron acceptor and the effect of that on an ICT/TICT state. The H-bonding with the electron acceptor increases the flow of charge from donor-to-acceptor, and therefore, it should favor the ICT process. In this experiment, ADMQ shows a similar amount of red shift (538–549 nm) of fluorescence maxima but with a moderate fluorescence quenching. The quenching efficiency is much lower than that of protic polar ethanol as it is calculated from the Stern–Volmer quenching plot shown in the inset of Figure 2. So the ICT-to-TICT conversion also exists in aprotic polar solvents but to a lower extent. In alcohol, ICT-to-TICT conversion is faster than that of ACN, hence it may be concluded that ICT in ADMQ is facilitated by strengthening the H-bond in the TICT state. However, for ADMQ, the intermolecular H-bonding-induced radiationless transition in alcohols competes with TICT emission.

Hard–Soft Ionic Character of E.S. This radiationless deactivation may also be explained by Hard–Soft anionic character of the excited state. In accordance with the hard soft acid base (HSAB) theory alkylamine or hydroxide ion, a hard base has its negative charge localized on a specific atom with high electronegativity, whereas benzene is a typical soft base in which the electrons are delocalized.[30] In Figure 1e, ADMQ shows the complete charge transfer that has occurred from the donor to the acceptor moiety, the quinoline ring gets an extra charge in the E.S due to TICT, so the dipole–dipole interaction between the quinoline ring and the alcohol may play an important role, as probably indicated by substantial red shift in the fluorescence spectra. However, the dipole–dipole interaction competes with the H-bonding interaction between the oxygen atom of the molecule and the alcohol. The time-resolved fluorescence and absorption studies will be performed in our future work to explore the mode of (in-plane and/or out-plane mode with respect to the molecular plane) H-bonding possibilities in detail.

Solvation in Water. *Structural Change of ADMQ in Water.* The solvation in water has been explored to identify the exact behavior of the newly designed ADMQ molecule in physiological condition. In water (pH = 7), lowest energy absorption band of ADMQ shows 15 nm shift toward higher wavelength without any appreciable change in the emission maxima (exciting at the same band) as compared to methanol (absorption band appears at 419 nm in methanol and 434 nm in water). This is explained as the electronegative oxygen in the ADMQ molecule is strongly H-bonded with water and gets protonated; the consequent structural change occurs as shown in Scheme 3.

In ADMQ, the conjugated double bond in enone part is activated by the presence of the carbonyl group. In water, once the carbonyl oxygen is strongly H-bonded and gets protonated, it creates an electrophilic center on the β-carbon, another −OH group from the solvent molecule attacks this carbon center resulting in a β-hydroxy compound with the loss in conjugation and hence the ICT becomes completely stopped. The emission maxima position remains unchanged as the molecule has lost its conjugation, so there is no possibility of ICT and ICT-to-TICT conversion in the E.S. Hence, ADMQ undergoes structural changes from its native structure to another stable β-hydroxy form (form-III, Scheme 3) in water. However, a dynamic equilibrium may exist between the β-hydroxy ADMQ and a resonance-stabilized enolate ion (form-IV, Scheme 3). Alkoxide ion being less nucleophilic than OH^-, the possibility of similar saturated keto compound in alcohol is probably less. These phenomena have got their confirmation by the FTIR studies of ADMQ in water when compared with other solvents.

FTIR studies reveal that ketone shows a very strong band for the C═O group that appears in the range of 1720–1708 cm^{-1} for simple aliphatic ketones, and the band is shifted toward lower frequency 1670–1600 cm^{-1} when the C═O group is in conjugation with aromatic rings on both sides.[24] ADMQ has shown the C═O peak at around 1633 cm^{-1} in aprotic polar ACN. Interestingly this C═O band (1633 cm^{-1}) disappeared when the molecule is dissolved in the isopropyl alcohol and a new broad peak has appeared at 3352 cm^{-1}, could be of H-bonded carbonyl (C═O···H) group peak as reported for other molecules.[33] Moreover, the same peak at 3352 cm^{-1} is absent when ADMQ is dissolved in aprotic polar ACN solvent; hence, in alcohol the carbonyl oxygen of ADMQ is H-bonded in the G.S., as described in an earlier section. In water, the carbonyl peak at 1633 cm^{-1} again reappears back with a broad −OH peak at 3230–3570 cm^{-1} as carbonyl and −OH groups both are present in the β-hydroxy carbonyl compound. FTIR studies confirm that ADMQ undergo structural change from its native structure to a β-hydroxy form in water and this information could be very useful to assess the mechanistic details of the chalcone derivatives in physiological conditions for their therapeutic applications.

Quantum Mechanical Calculations for β-Hydroxy Keto Compound. In water, all possible structural variants have been examined theoretically to rationalize the experimental observations. The G.S. geometries of form II, where the oxygen of the keto group gets H-bonded with the water, saturated β-hydroxy keto compound (form III), and the enolate

dx.doi.org/10.1021/jp5025262 | J. Phys. Chem. B XXXX, XXX, XXX–XXX

ion (form IV) have been studied in detail by the DFT/B3LYP level. The HOMO−LUMO gap is found to be lower (2.73 eV) in the H-bonded species (form II) than the original native compound (form I), while in case form III, the value is maximum (3.49 eV). The possible UV−vis peak positions of chloro analogues of forms II, III, and IV have been studied by ZINDO−CI and ZINDO-RPA methods and documented in Table 1. It suggests that the red-shifted absorption band in water is probably due to the H-bonded species (form II) with possible low-intensity absorption by the saturated β-hydroxy keto compound near 350 nm (confirmed experimentally by excitation spectra in water). So the possibility of both H-bonded ADMQ and saturated β-hydroxy keto form may exist simultaneously in water with a dynamic equilibrium between these two. Hence, theoretical results support the FTIR findings for the existence of the β-hydroxy keto form of ADMQ. The saturated form III does not have charge transfer property as evidenced by its nature of HOMO and LUMO (S2).

Cytotoxicity Screening Report of ADMQ. The compound ADMQ does not show minimum inhibitory concentration (MIC) in the concentrations tested against the *E. coli AB 1157* cells. This suggests that the compound does not exhibit any deleterious effect or toxicity to the *E. coli* strain in study, while in control experiment stannous chloride (has been used as a standard), a toxic chemical which induces free-radical-mediated lethality shows an MIC of 0.25 mg (S3). These data implicate that ADMQ does not exhibit cytotoxic effects in *E. coli AB 1157* cells in a dose-dependent manner.

DNA Damage by Synthesized ADMQ. *Agarose Gel Electrophoresis.* A large number of small molecules like ADMQ, including some of clinical value, induce DNA damage either directly by cleavage of DNA[34] or by alkylation[35] or indirectly via inhibition of topoisomerase activities.[36] The interaction of ADMQ with DNA has been studied to identify the structural changes in the DNA, such as bending, winding, or strand breaking, which may result in DNA damage through inhibition or regulation of DNA replication and transcription. The interaction of ADMQ with ct DNA in the 50 mM HEPES buffer at pH 7 has been examined by the agarose gel electrophoresis study.[37] It has shown the cleavage of DNA at all concentrations of ADMQ as indicated by smear of cleaved ct DNA at multiple positions as compared with the untreated ct DNA (Figure 3a). Such a cleavage pattern is consistent with distributive nature of ADMQ.

Molecular Dynamics Simulation. MD simulation has been carried out to corroborate and to explain the gel electrophoresis findings. Prior to MD simulation, all possible forms of ADMQ have been docked with DNA (PDB ID: 226D) and compared on the basis of GLIDE score and MM-GBSA binding energy. Form II has shown the highest binding energy (−41.7209 kcal/mol) and GLIDE score (−4.8704). The best pose of ADMQ (form II) generated by molecular docking study with DNA is considered for the explicit MD simulation by Desmond,[38] where system builder used explicit aqueous medium followed by complex minimization to bring down energy to the lowest energy level. The ligand−DNA complex real time simulation of 10 ns clarifies the ligand stability and the interaction pattern with the double helical DNA. It shows that ADMQ forms H-bond with the deoxyribose sugar attached with the nucleobase adenine DA-17 of chain A (Figure 3b). The H-bond acts as an anchor, determining the specific position of the ligand along with hydrophobic influence of adenine and thymine nucleobases available in the vicinity. Moreover the molecular docking

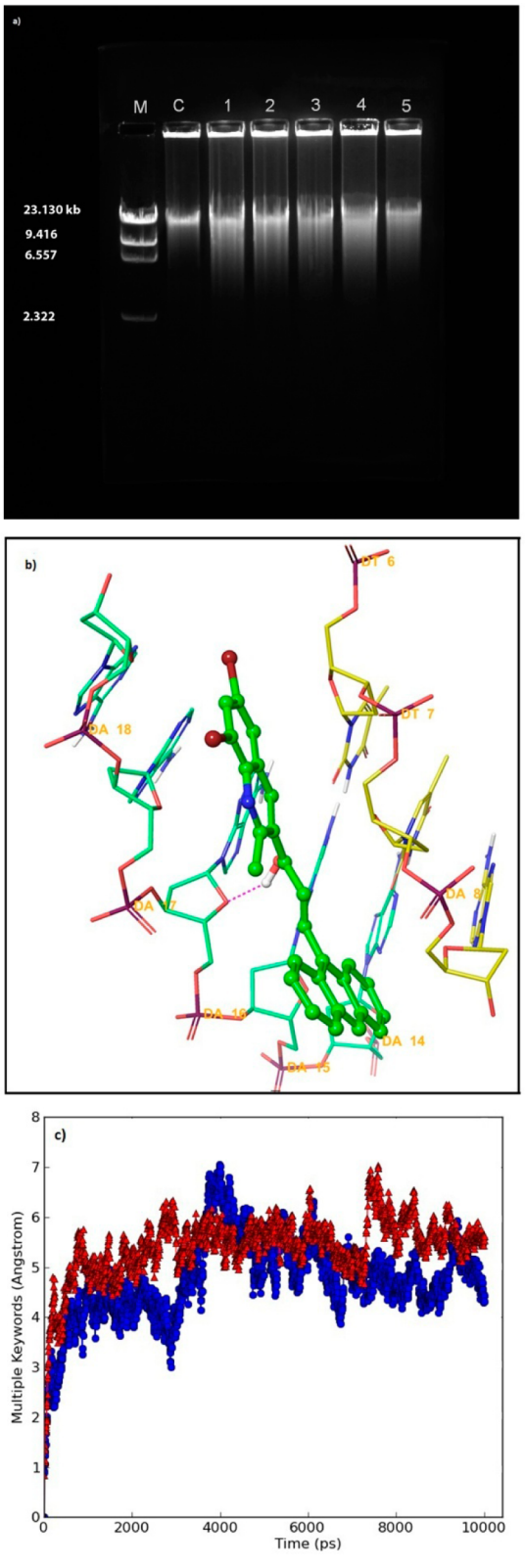

Figure 3. (a) ADMQ-induced cleavage of ct DNA. M, standard DNA molecular weight marker (λ DNA *Eco*RI/*Hin*dIII double digest); C, control DNA (untreated sample), 1−5-DNA treated with 10, 25, 50, 75, and 100 μg of sample, respectively. (b) Close-up view of ADMQ-DNA binding through H-bond with the deoxyribose sugar attached with nucleobase DA-17 (shown in pink). (c) RMSD plot of the trajectory for the ADMQ (blue) and EtBr (red) complex against DNA.

dx.doi.org/10.1021/jp5025262 | J. Phys. Chem. B XXXX, XXX, XXX−XXX

of β-hydroxy keto form (form III) also shows H-bond interaction with the same deoxyribose sugar attached with the nucleobase adenine DA-17. The MD trajectory depicts that ADMQ acquires a crescent shape while entering into the DNA structure, and the quinoline moiety enters into the DNA with the anthracene part exposed outside the surface of sugar phosphate backbone. The DNA base pairs probably become widened at the binding site in ADMQ-conjugated DNA structure to accommodate it in sequence specific manner.

This H-bonding, hydrophobic interactions, and van der Waals forces support the binding with the nucleic acid, resulting in a significant structural change in DNA which perhaps potentially leads to DNA strand breaking/cleavage as noticed in the agarose gel electrophoresis experiment.

In addition, the ligand stability has also been examined and compared by the MD simulation with ethidium bromide (EtBr)−DNA complex and supported by the RMSD plot (Figure 3c). The RMSD pattern averaging overall RMSD of around 6 Å reflects the comparable stability of the synthesized molecule with EtBr at an atomic scale level.

The detail DNA binding mode[2,4,39] (electrostatic, groove or intercalation) of ADMQ will be explored by various experiments like fluorescence anisotropy, control fluorescence quenching in the presence of iodide ion, helix melting, viscometry, comparative binding with EtBr, FTIR studies, and circular dichromism study in our next article.

CONCLUSION

A bioactive quinoline-appended chalcone derivative, (*E*)-3-(anthracen-10-yl)-1-(6,8-dibromo-2-methylquinolin-3-yl)prop-2-en-1-one, expected to possess an anticancer, antitumor, and other important therapeutic activities of significant potency with low systematic toxicity has been designed and synthesized. A dual emission has been observed from LE and TICT state with different photophysical behavior in aprotic and protic polar solvents. Radiationless deactivation of the excited states has been identified and found to be promoted strongly by hydrogen bonding. The compound acts as a molecular rotor which undergoes an intramolecular twist in the excited state, resulting in a complete charge transfer from the anthracene (donor) to quinoline (acceptor) via enone linker. The molecule undergoes a major structural change from its native structure to a β-hydroxy carbonyl compound when administered in the physiological environment. This may be extremely useful for its delivery and therapeutic applications. ADMQ strongly interacts with DNA through H-bonding with the deoxyribose sugar attached with the nucleobase DA-17 of chain A of DNA and causes a significant structural change that potentially cleave the DNA double helix. The compound does not exhibit any deleterious effect or toxicity to the *E. coli* strain in cytotoxicity studies. The consolidated spectroscopic research described herein signifies a promising approach, exemplifying a novel use of quinoline-appended chalcone derivative and their interaction with relevant target nucleic acids. We can envision this to open up new avenues for screening and designing of suitable chalcone-based therapeutic agents to control the gene expression for medicinal chemistry research in academia as well is industry.

ASSOCIATED CONTENT

Supporting Information

Figure S1: Design and molecular docking of chalcone derivatives; Figure S2: HOMO and LUMO diagrams of the saturated β-hydroxyketo compound and H-bonded ADMQ; and Figure S3: cytotoxicity report. This material is available free of charge via the Internet at http://pubs.acs.org.

AUTHOR INFORMATION

Corresponding Author

*E-mail: sujitju@yahoo.co.in and skghosh@chm.vnit.ac.in. Tel: +(91) 712 2801775. Fax: + (91) 712-2223230/2801357.

Notes

The authors declare no competing financial interest.

ACKNOWLEDGMENTS

CSIR Financial support scheme no. 37 (1493)11/EMR-II is gratefully acknowledged. Author thanks Schrödinger for providing Glide 9.3 module evaluation licence. Author gives thanks to Prof. N. Chattopadhyay, Dept. of Chemistry, Jadavpur University for giving opportunity for lifetime measurements. We would also like to thank respected anonymous reviewers for their critical comments and suggestions.

REFERENCES

(1) Kumar, A.; Alegria, A. E. Synthesis of Novel Functionalized 4-Aza-2,3-Didehydropodophyllotoxin Derivatives with Potential Anti-tumor Activity. *J. Heterocycl. Chem.* **2010**, *47*, 1275−1282.

(2) Mati, S. S.; Roy, S. S.; Chall, S.; Bhattacharya, S.; Bhattacharya, S. C. Unveiling the Groove Binding Mechanism of a Biocompatible Naphthalimide-Based Organoselenocyanate with Calf Thymus DNA: An "Ex Vivo" Fluorescence Imaging Application Appended by Biophysical Experiments and Molecular Docking Simulations. *J. Phys. Chem. B* **2013**, *117*, 14655−14665.

(3) Hossain, U. Sk.; Prakasha, G. P.; Crampsie, M. A.; Yun, J. K.; Spratt, T. E.; Amin, S.; Sharma, A. K. Development of Novel Naphthalimide Derivatives and their Evaluation as Potential Melanoma Therapeutics. *Eur. Med. Chem.* **2011**, *46*, 3331−3338.

(4) Jana, B.; Senapati, S.; Ghosh, D.; Bose, D.; Chattopadhyay, N. Spectroscopic Exploration of Mode of Binding of ct DNA with 3-Hydroxyflavone: A Contrast to the Mode of Binding with Flavonoids Having Additional Hydroxyl Groups. *J. Phys. Chem. B* **2012**, *116*, 639−645.

(5) Jaffer, S. S.; Ghosh, P.; Purkayastha, P. Mechanistic Pathway for Controlled Extraction of Guest Molecule Bound to Herring Sperm DNA Using α-Cyclodextrin. *Spectrochim. Acta, Part A* **2011**, *78*, 1587−1591.

(6) Batovska, D. I.; Todorova, I. T. Trends in Utilization of the Pharmacological Potential of Chalcones. *Curr. Clin. Pharmacol.* **2010**, *5*, 1−29.

(7) Kumar, D.; Kumar, N. M.; Akamatsu, K.; Kusaka, E.; Harada, H.; Ito, T. Synthesis and Biological Evaluation of Indolyl Chalcones as Antitumor Agents. *Bioorg. Med. Chem. Lett.* **2010**, *20*, 3916−3919.

(8) Konieczny, M. T.; Konieczny, W.; Sabisz, M.; Skladanowski, A.; Wakiec, R.; Augustynowicz-Kopec, E.; Zwolska, Z. Acid-Catalyzed Synthesis of Oxathiolone Fused Chalcones. Comparison of their Activity Toward Various Microorganisms and Human Cancer Cells Line. *Eur. J. Med. Chem.* **2007**, *42*, 729−733.

(9) Liu, M.; Wilairat, P.; Go, M. L. Antimalarial Alkoxylated and Hydroxylated Chalcones: Structure-Activity Relationship Analysis. *J. Med. Chem.* **2001**, *44*, 4443−4452.

(10) Edenharder, R.; Petersdorff, I. V.; Rauscher, R. Antimutagenic Effects of Flavonoids, Chalcones and Structurally Related Compounds on the Activity of 2-Amino-3-Methylinidazo [4,5-*f*] Quinoline (IQ) and Other Heterocyclic Amine Mutagens from Cooked Food. *Mutat. Res.* **1993**, *287*, 261−274.

(11) Datta, J.; Ghoshal, K.; Denny, W. A.; Gamage, S. A.; Brooke, D. G.; Phiasivongsa, P.; Redkar, S.; Jacob, S. T. A New Class of Quinoline-Based DNA Hypomethylating Agents Reactivates Tumor

Suppressor Genes by Blocking DNA Methyltransferase 1 Activity and Inducing its Degradation. *Cancer Res.* **2009**, *69*, 4277−4285.
(12) Vijay, K.; Ganapathy, S.; Adapa, S. R. Synthesis of a New Series of Quinolinyl Chalcones as Anticancer and Anti-inflammatory Agents. *Indian J. Chem.* **2010**, *49*, 1109−1116.
(13) Xinwei, L.; Daohang, H. Synthesis and Optical Properties of Novel Anthracene-Based Stilbene Derivatives Containing an 1, 3, 4-Oxadiazole Unit. *Dyes Pigm.* **2012**, *93*, 1422−1427.
(14) Fayed, T. A.; Awad, M. K. Dual Emission of Chalcone-Analogue Dyes Emitting in the Red Region. *Chem. Phys.* **2004**, *303*, 317−326.
(15) Prasath, R.; Bhavana, P.; Ng, S. W.; Tiekink, E. R. T. The Facile and Efficient Ultrasound-Assisted Synthesis of New Quinoline-Appended Ferrocenyl Chalcones and their Properties. *J. Organomet. Chem.* **2013**, *726*, 62−70. et al. 1-(6,8-Dibromo-2-Methylquinolin-3-yl)ethanone, *Acta Crystallogr.* **2011**, *E67*, o2664, 10.1107/S1600536811037044.
(16) Haidekker, M. A.; Theodorakis, E. A. Environment-Sensitive Behavior of Fluorescent Molecular Rotors, *J. Biol. Eng.* **2010**, *4*, 11, 10.1186/1754-1611-4-11.
(17) Hobeika, N.; Malval, J.-P.; Chaumeil, H.; Roucoules, V.; Morlet-Savary, F.; Nouen, D. L.; Gritti, F. Abnormal Enhancement of the Photoisomerization Process in a Trans-Nitroalkoxystilbene Dimer Sequestered in *β*-Cyclodextrin Cavities. *J. Phys. Chem. A* **2012**, *116*, 10328−10337.
(18) Leydet, Y.; Batat, P.; Jonusauskas, G.; Denisov, S.; Lima, J. C.; Parola, A. J.; McClenaghan, N. D.; Pina, F. Impact of Water on the Cis−Trans Photoisomerization of Hydroxychalcones. *J. Phys. Chem. A* **2013**, *117*, 4167−4173.
(19) Dodiuk, H.; Kosower, E. M. Multiple Fluorescences. 4. The Protonated Form of *N*-alkyl-2-*N*-arylamino-6-naphthalenesulfonates. *J. Am. Chem. Soc.* **1977**, *99*, 859−865.
(20) Kosower, E. M. Intramolecular Donor-Acceptor Systems. 9. Photophysics of (Phenylamino)naphthalenesulfonates: A Paradigm for Excited−State Intramolecular Charge Transfer. *Acc. Chem. Res.* **1982**, *15*, 259−266.
(21) Rotkiewicz, K.; Grellmann, K. H.; Grabowski, Z. R. Reinterpretation of the Anomalous Fluorescence of p-n,n-dimethylaminobenzonitrile. *Chem. Phys. Lett.* **1973**, *19*, 315−318.
(22) Grabowski, Z. R.; Rotkiewicz, K. Structural Changes Accompanying Intramolecular Electron Transfer: Focus on Twisted Intramolecular Charge-Transfer States and Structures. *Chem. Rev.* **2003**, *103*, 3899−4031.
(23) Nad, S.; Kumbhakar, M.; Pal, H. Photophysical Properties of Coumarin-152 and Coumarin-481 Dyes: Unusual Behavior in Nonpolar and in Higher Polarity Solvents. *J. Phys. Chem. A* **2003**, *107*, 4808−4816.
(24) Nad, S.; Pal, H. Unusual Photophysical Properties of Coumarin-151. *J. Phys. Chem. A* **2001**, *105*, 1097−1106.
(25) Han, K.-Li; Zhao, G.-J. Ultrafast Hydrogen Bond Strengthening of the Photoexcited Fluorenone in Alcohols for Facilitating the Fluorescence Quenching. *J. Phys. Chem. A* **2007**, *111*, 9218−9223.
(26) Biczok, L.; Berces, T.; Linschitz, H. Quenching Processes in Hydrogen-Bonded Pairs: Interactions of Excited Fluorenone with Alcohols and Phenols. *J. Am. Chem. Soc.* **1997**, *119*, 11071−11077.
(27) Barman, N.; Singha, D.; Sahu, K. Fluorescence Quenching of Hydrogen-Bonded Coumarin 102-Phenol Complex: Effect of Excited-State Hydrogen Bonding Strength. *J. Phys. Chem. A* **2013**, *117*, 3945−3953.
(28) Chipem, F. A. S.; Mishra, A.; Krishnamoorthy, G. The Role of Hydrogen Bonding in Excited State Intramolecular Charge Transfer. *Phys. Chem. Chem. Phys.* **2012**, *14*, 8775−8790.
(29) Gregoire, G.; Dimicoli, I.; Mons, M.; Donder-Lardeux, C.; Jouvet, C.; Martrenchard, S.; Solgadi, D. Femtosecond Dynamics of TICT State Formation in Small Clusters: The Dimethylaminobenzomethyl Ester Acetonitrile System. *J. Phys. Chem. A* **1998**, *102*, 7896−7902.
(30) Morimoito, A.; Yatsuhashi, T.; Shimada, T.; Biczok, L.; Tryk, D. A.; Inoue, H. Radiationless Deactivation of an Intramolecular Charge Transfer Excited State Through Hydrogen Bonding: Effect of Molecular Structure and Hard-Soft Anionic Character in the Excited State. *J. Phys. Chem. A* **2001**, *105*, 10488−10496.
(31) Morimoito, A.; Biczok, L.; Yatsuhashi, T.; Shimada, T.; Baba, S.; Tachibana, H.; Tryk, D. A.; Inoue, H. Radiationless Deactivation of an Intramolecular Charge Transfer Excited State Through Hydrogen Bonding: Effect of Molecular Structure and Hard-Soft Anionic Character in the Excited State. *J. Phys. Chem. A* **2002**, *106*, 10089−10095.
(32) Saha, S. K.; Purkayastha, P.; Das, A. B. Photophysical Characterization and Effect of pH on the Twisted Intramolecular Charge Transfer Fluorescence of Trans-2-[4 (dimethylamino)styryl]-benzothiazole. *J. Photochem. Photobiol., A* **2008**, *195*, 368−377.
(33) Pavia, D. L.; Lampman, G. M.; Kriz, G. S.; Vyvyan, J. R. *Introduction to Spectroscopy*, 4th ed.; Brooks/Cole: Belmont, CA, 2009.
(34) Yesuthangam, Y.; Pandian, S.; Venkatesan, K.; Gandhidasan, R.; Murugesan, R. Photogeneration of Reactive Oxygen Species and Photoinduced Plasmid DNA Cleavage by Novel Synthetic Chalcones. *J. Photochem. Photobiol., B* **2011**, *102*, 200−208.
(35) Sirajuddin, M.; Ali, S.; Badshah, A. Drug−DNA Interactions and their Study by UV−Visible, Fluorescence Spectroscopies and Cyclic Voltametry. *J. Photochem. Photobiol., B* **2013**, *124*, 1−19.
(36) Bailly, C.; Chaires, J. B. Sequence Specific DNA Minor Groove Binders. Design and Synthesis of Netropsin and Distamycin Analogues. *Bioconjugate Chem.* **1998**, *9*, 513−538.
(37) Sambrook, J.; Fritsch, E. F.; Maniatis, T. *Molecular Cloning, A Laboratory Manual*, 2nd ed.; Cold Spring Harbor Laboratory; Cold Spring Harbor, New York, 1989.
(38) Friesner, R. A.; Banks, J. L.; Murphy, R. B.; Halgren, T. A.; Klicic, J. J.; Mainz, D. T.; Repasky, M. P.; Knoll, E. H.; Shaw, D. E.; Shelley, M.; et al. A New Approach for Rapid, Accurate Docking and Scoring. 1. Method and Assessment of Docking Accuracy. *J. Med. Chem.* **2004**, *47*, 1739−1749.
(39) Mukherjee, A.; Lavery, R.; Bagchi, B.; Hynes, J. T. On the Molecular Mechanism of Drug Intercalation into DNA: A Simulation Study of the Intercalation Pathway, Free Energy, and DNA Structural Changes. *J. Am. Chem. Soc.* **2008**, *130*, 9747−9755.